

Supplementary Information

Redox reaction does not facilitate oxygen evolution on bismuth ruthenate pyrochlore

Joohyuk Park,^{*a} Haeseong Jang,^a Su Yong Lee,^a Jeong Suk Jeon^a and Min Gyu Kim^{*a}

^aPLS-II Beamline Division, PLS-II Department, Pohang Accelerator Laboratory (PAL), Pohang University of Science and Technology (POSTECH), Pohang, Gyeongbuk 37673, Republic of Korea

*E-mail: jhpark20@postech.ac.kr; mgkim@postech.ac.kr

1. Experimental Section

Preparation of electrocatalyst. To prepare the bismuth ruthenate pyrochlore oxide ($\text{Bi}_2\text{Ru}_2\text{O}_7$), a buffer solution was required. The buffer solution, NH_4 -EDTA, was made with a mixture of 10 g anhydrous ethylenediaminetetraacetic acid ($\geq 99\%$ titration, Sigma-Aldrich), 1 M ammonia solution (28.0~30.0%, Samchun chemical), and 1.5 ml nitric acid (HNO_3 , ACS reagent 70%, Sigma-Aldrich) at a solution pH of 7. To prepare the $\text{Bi}_2\text{Ru}_2\text{O}_7$, 8.22×10^{-4} mol bismuth (III) nitrate pentahydrate (reagent grade 98%, Sigma-Aldrich), 8.22×10^{-4} mol ruthenium (III) nitrosyl nitrate solution (1.5 wt% Ru, Sigma-Aldrich) and 10 g anhydrous citric acid (99%, Sigma-Aldrich) were dissolved and stirred with the buffer solution for 24 h at 150 °C. At this point, gelation was observed. The gelled solution was transferred to an oven at 200 °C for 6 h drying. The prepared powder was calcined in a muffle furnace at 1,050 °C for 5 h under static air.

Preparation of working electrode. The catalyst inks were prepared with mixture of 16 mg of the $\text{Bi}_2\text{Ru}_2\text{O}_7$ powder, 4 mg of ketjenblack carbon (EC 600JD), 200 μl of the 5 wt% of Nafion in mixture of lower aliphatic alcohols and H_2O (Sigma-Aldrich), and 800 μl of ethanol. Briefly, the catalyst inks were prepared by ultrasonically mixing in distilled water for 1 h to make homogeneous mixture. The portion of 5 μl of inks were loaded on the glassy carbon of rotation ring disk electrode (RRDE) as the working electrode. The area of RRDE was 0.1256 cm^2 . As a result, the loading levels of the prepared pyrochlore oxide was 0.637 $\text{mg}_{\text{cat}} \text{cm}^{-2}$. For the loading level of 0.637 $\text{mg}_{\text{IrO}_2} \text{cm}^{-2}$ benchmarking catalyst, 16 mg of IrO_2 powder and 4 mg of ketjenblack carbon (EC 600JD) was dispersed in 200 μl of the 5 wt% of Nafion solution and 800 μl of ethanol. After that, this catalyst ink was prepared by ultrasonically mixing in distilled water for at least 1 h to make homogeneous ink. Then, 5 μl of ink was loaded on the glassy carbon of working electrode that the loading level of IrO_2 was 0.637 $\text{mg}_{\text{IrO}_2} \text{cm}^{-2}$.

Electrochemical measurement. A three-electrode cell was used to measure the catalytic activities of $\text{Bi}_2\text{Ru}_2\text{O}_7$. The rotating ring disk electrode (RRDE) (ALS Co., Ltd) tests were carried out based on the pyrochlore catalysts film (loaded on the glassy carbon of RRDE) for the working electrode in O_2 -saturated 0.1 M KOH alkaline electrolyte. Platinum wire and Hg/HgO were used as the counter and reference electrodes, respectively. Electrochemical characterizations were conducted using a bipotentiostat (IviumStat). The scan rate of 10 mV s^{-1} was swept from 1.23 to 1.82 V versus RHE for oxygen evolution reaction (OER). The CVs were capacitive-corrected by averaging current of the forward and backward sweeps. The capacitive-corrected currents were ohmically corrected with the measured ionic resistance ($\approx 45 \Omega$).

In situ XAS analysis. In situ XAS was conducted on the multipole-wiggler BL10C beamline (Wide XAFS) at the Pohang Light Source-II (PLS-II) with top-up mode operation under a ring current of 250 mA at 3.0 GeV. Monochromatic X-ray beams were obtained with a liquid nitrogen cooled double crystal monochromator (Bruker ASC) with available in situ exchange in vacuum between a Si(111) and Si(311) crystal pair. In this study, the Si(111) crystal pair was used for bismuth and ruthenium ions of $\text{Bi}_2\text{Ru}_2\text{O}_7$ during in situ XAS analysis. An three-electrode electrochemical cell was assembled for in situ XAS analysis, which consists of working electrode with $\text{Bi}_2\text{Ru}_2\text{O}_7$, reference electrode based on Hg/HgO and platinum wire as a counter electrode. Electrochemical characterizations were conducted simultaneously with in situ XAS analysis in transmittance and fluorescence modes using N_2 gas-filled ionization chambers (IC-SPEC, FMB Oxford) for incident X-ray photons and passivated implanted planar silicon (PIPS) detector for the fluorescent X-ray photons. In order to eliminate higher-order harmonic contaminations, the intensity of incident X-ray has been detuned to reduce by $\sim 30\%$. Energy calibration processes were conducted for each XAS measurement with reference foils placed in front of third ion

chamber. On the basis of standard XAS analysis, reductions of obtained spectra were performed into the normalized XANES and Fourier-transformed radial distribution functions (RDF). AUTOBK and FEFFIT modules in UWXAFS package were used to obtain the k^2 -weighted ruthenium K-edge and bismuth L_3 -edge EXAFS spectra with the removal of background and normalization processes on the edge jump. The $k^2\chi(k)$ spectra were Fourier-transformed in k range from 2.5 to 13.5 \AA^{-1} and from 3 to 12.5 \AA^{-1} for ruthenium and bismuth ions, respectively.

Material characterization. The crystal structure of $\text{Bi}_2\text{Ru}_2\text{O}_7$ was analyzed by using XRD on BL8D beamline (XRS POSCO) at the PLS-II with top-up mode operation under a ring current of 250 mA at 3.0 GeV. XRD was performed in the range of $10^\circ \leq 2\theta \leq 70^\circ$ with a step size of 0.04° . The material morphology was examined using high-resolution scanning electron microscopy (SEM) (JSM 7401F, JEOL).

2. Supplementary Figures

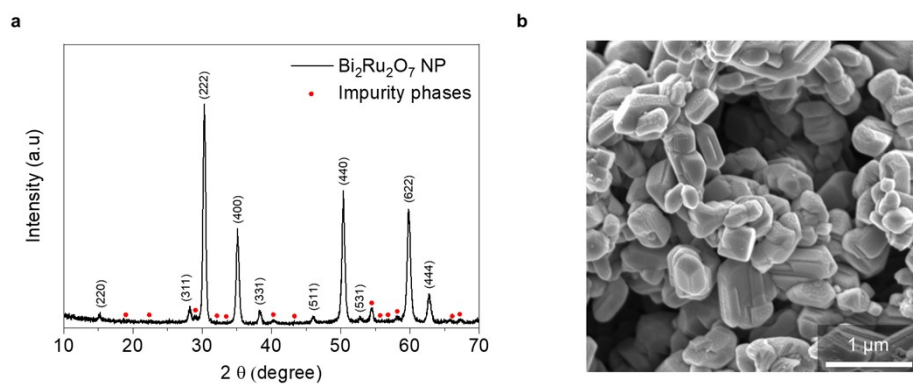


Fig. S1 (a) XRD pattern and (b) SEM image of $\text{Bi}_2\text{Ru}_2\text{O}_7$ nanoparticles with impurities.

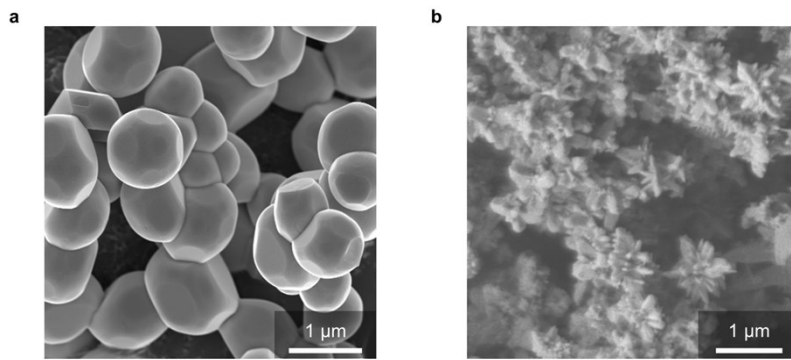


Fig. S2 (a) SEM images of micrometer-sized $\text{Bi}_2\text{Ru}_2\text{O}_7$ and (b) state-of-the-art IrO_2 nanoparticles as electrocatalysts for OER.

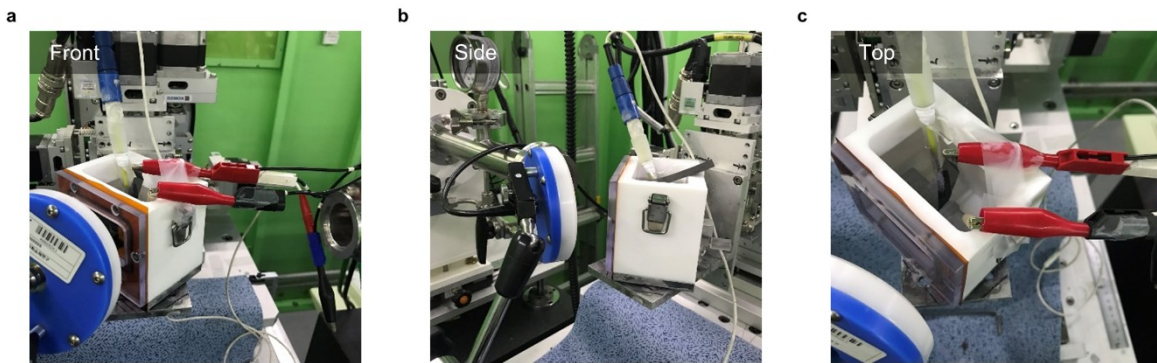


Fig. S3 (a) Photographs of three-electrode electrochemical cell for in situ XAS analysis at the front, (b) side and (c) top.

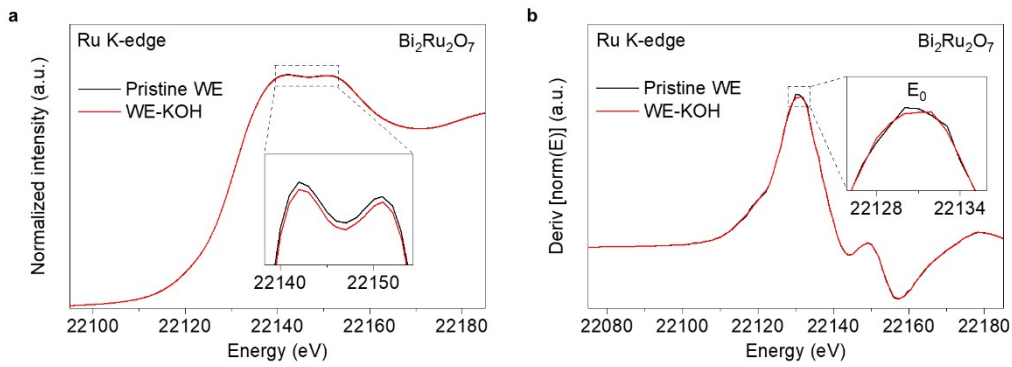


Fig. S4 XANES spectra of $\text{Bi}_2\text{Ru}_2\text{O}_7$ in working electrode of three-electrode electrochemical cell by ex situ XAS analysis for exploring redox reaction of ruthenium ions. (a) Normalized ruthenium K-edge XANES spectra of $\text{Bi}_2\text{Ru}_2\text{O}_7$ in pristine working electrode and working electrode with 0.1 M KOH electrolyte. (b) The first derivative ruthenium K-edge XANES spectra of $\text{Bi}_2\text{Ru}_2\text{O}_7$ in pristine WE and WE-KOH.

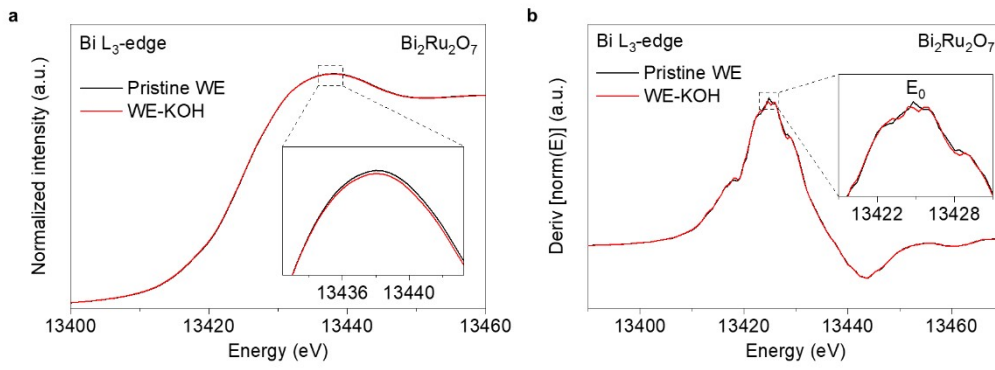


Fig. S5 XANES spectra of $\text{Bi}_2\text{Ru}_2\text{O}_7$ in working electrode of three-electrode electrochemical cell by ex situ XAS analysis for exploring redox reaction of bismuth ions. (a) Normalized bismuth L_3 -edge XANES spectra of $\text{Bi}_2\text{Ru}_2\text{O}_7$ in pristine working electrode and working electrode with 0.1 M KOH electrolyte. (b) The first derivative bismuth L_3 -edge XANES spectra of $\text{Bi}_2\text{Ru}_2\text{O}_7$ in pristine WE and WE-KOH.

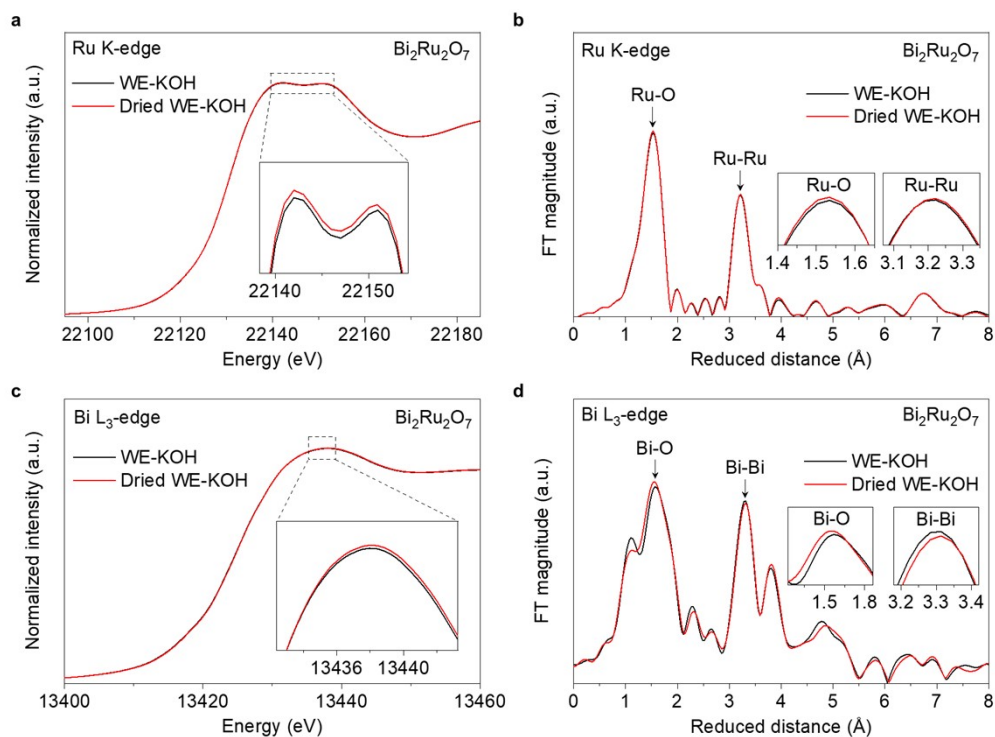


Fig. S6 (a) Normalized ruthenium K-edge XANES spectra and (b) normalized RDF of Fourier-transformed k^2 -weighted EXAFS spectra of $\text{Bi}_2\text{Ru}_2\text{O}_7$ in WE-KOH and dried WE-KOH with 0.1 M KOH electrolyte for ruthenium ions. (c) Normalized bismuth L_3 -edge XANES spectra and (d) normalized RDF of Fourier-transformed k^2 -weighted EXAFS spectra of $\text{Bi}_2\text{Ru}_2\text{O}_7$ in WE-KOH and dried WE-KOH with 0.1 M KOH electrolyte for bismuth ions.

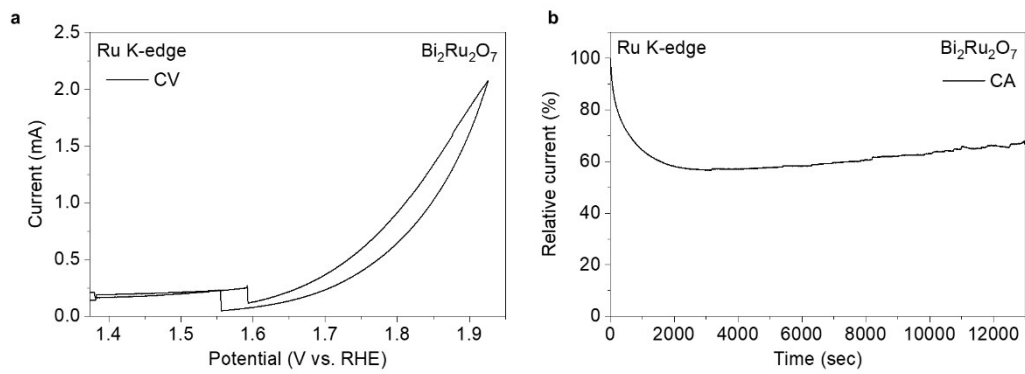


Fig. S7 (a) CV and (b) CA curves of $\text{Bi}_2\text{Ru}_2\text{O}_7$ in working electrode of three-electrode electrochemical cell at a potential of 1.7 V vs RHE simultaneously with XAS analysis for ruthenium ions during OER.

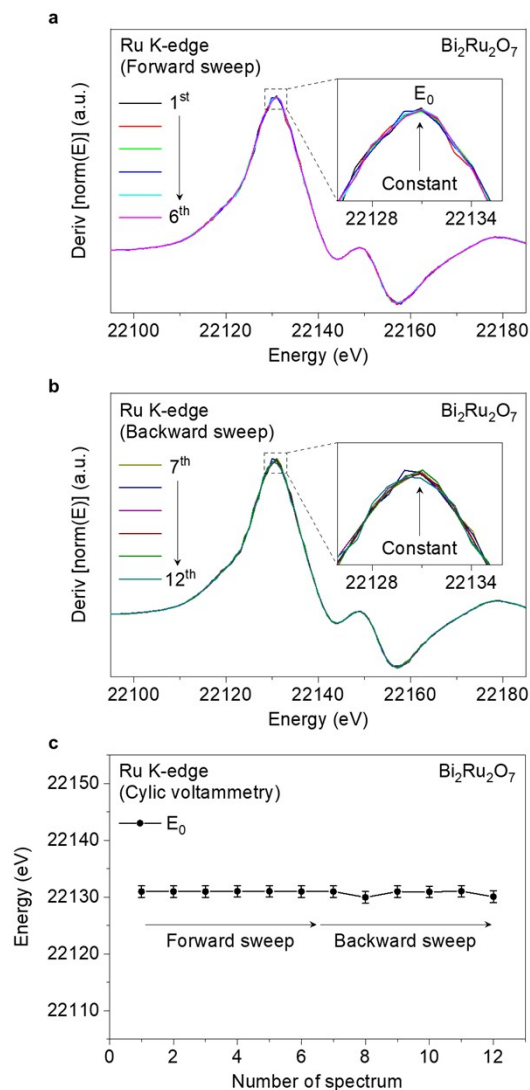


Fig. S8 (a) The first derivative ruthenium K-edge XANES spectra of $\text{Bi}_2\text{Ru}_2\text{O}_7$ during OER in the forward sweep and (b) backward sweep of CV test simultaneously with XAS analysis. The CV was recorded between 1.15 V to 1.7 V vs RHE. The scan number of XAS analysis for OER in the forward sweep ranged from 1st to 6th, and OER in the backward sweep from 7th to 12th. (c) E_0 of ruthenium K-edge XANES spectra of $\text{Bi}_2\text{Ru}_2\text{O}_7$ simultaneously with CV test.

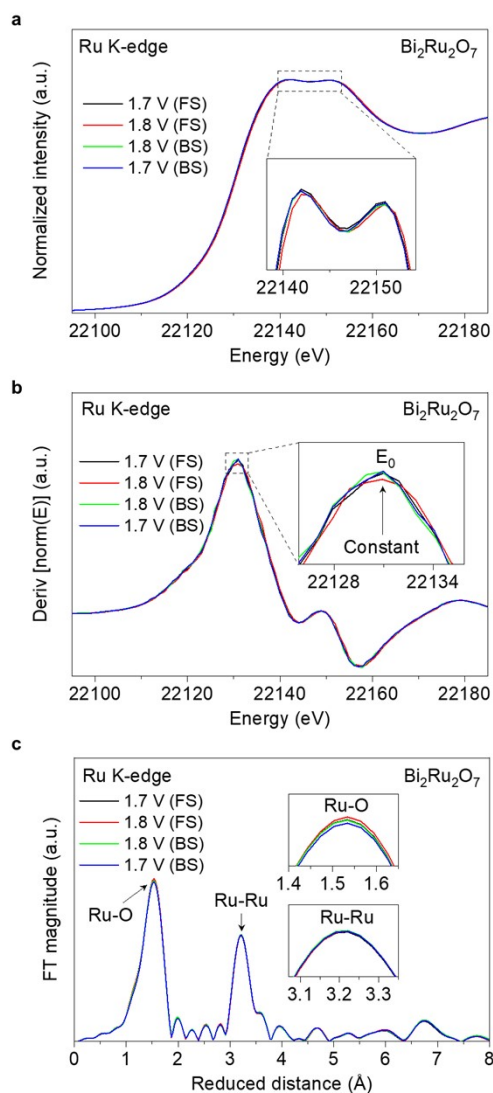


Fig. S9 (a) Normalized ruthenium K-edge XANES spectra, (b) the first derivative ruthenium K-edge XANES spectra and (c) normalized RDF of Fourier-transformed k^2 -weighted EXAFS spectra for ruthenium ions of $\text{Bi}_2\text{Ru}_2\text{O}_7$ at the high oxidative potentials during CV in the forward sweep (FS) and backward sweep (BS).

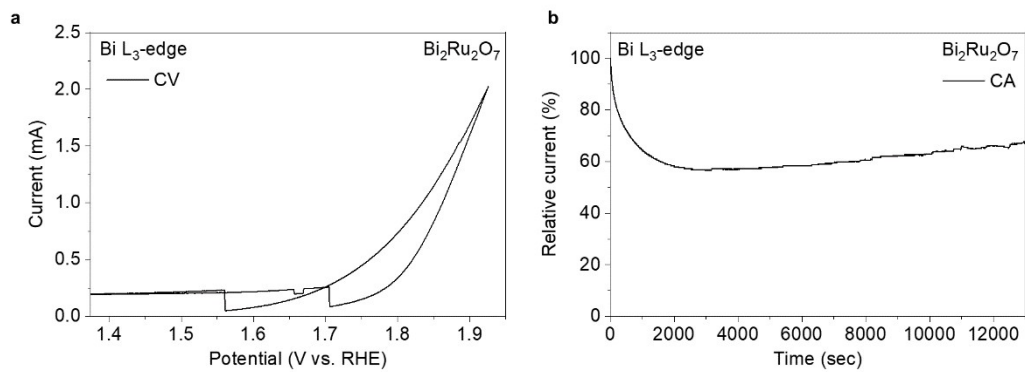


Fig. S10 (a) CV and (b) CA curves of Bi₂Ru₂O₇ in working electrode of three-electrode electrochemical cell at a potential of 1.7 V vs RHE simultaneously with XAS analysis for bismuth ions during OER.

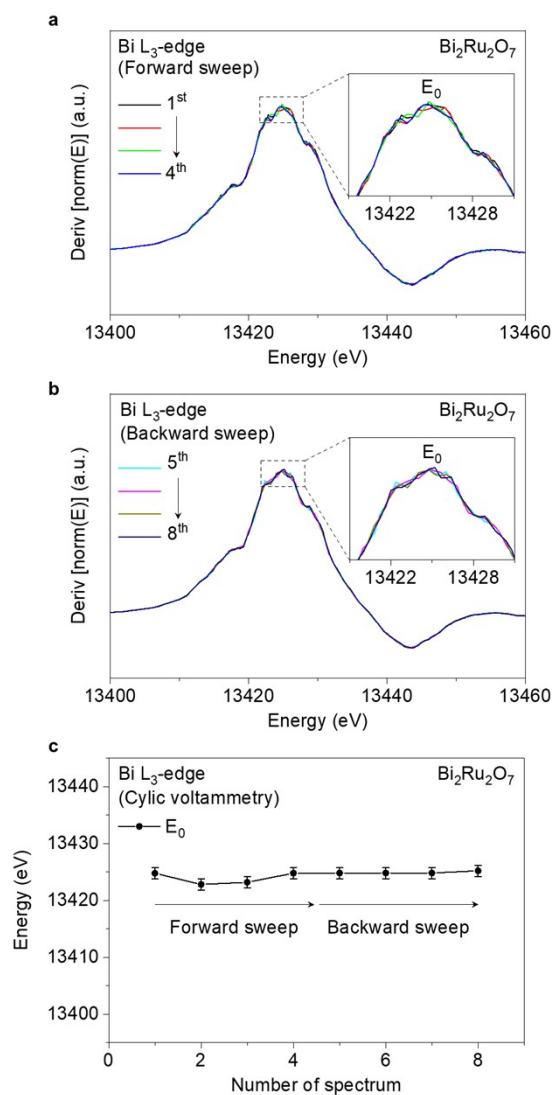


Fig. S11 (a) The first derivative bismuth L₃-edge XANES spectra of Bi₂Ru₂O₇ during OER in the forward sweep and (b) backward sweep of CV test simultaneously with XAS analysis. The CV was recorded between 1.15 V to 1.7 V vs RHE. The scan number of XAS analysis for OER in the forward sweep ranged from 1st to 4th, and OER in the backward sweep from 5th to 8th. (c) E₀ of bismuth L₃-edge XANES spectra of Bi₂Ru₂O₇ simultaneously with CV test.

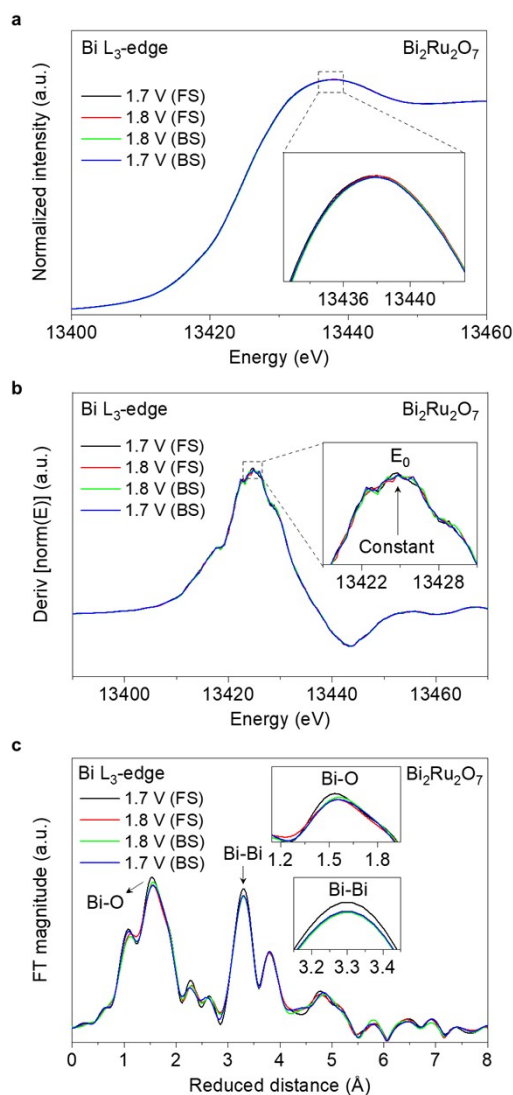


Fig. S12 (a) Normalized bismuth K-edge XANES spectra, (b) the first derivative bismuth K-edge XANES spectra and (c) normalized RDF of Fourier-transformed k^2 -weighted EXAFS spectra for bismuth ions of $\text{Bi}_2\text{Ru}_2\text{O}_7$ at the high oxidative potentials during CV in the forward sweep (FS) and backward sweep (BS).

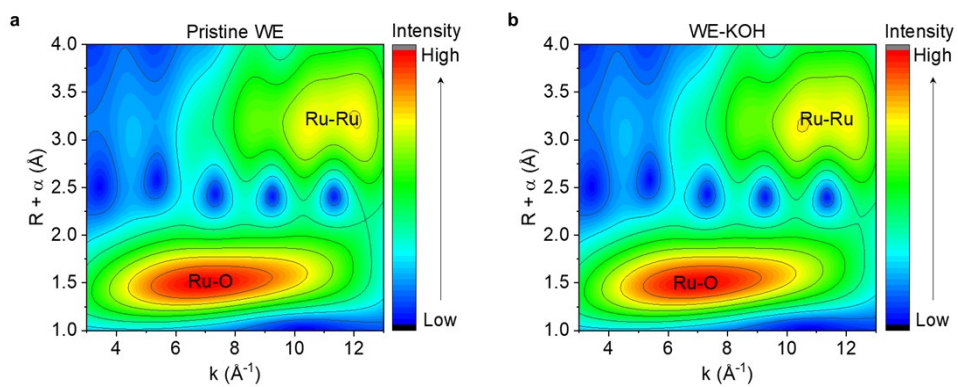


Fig. S13 (a) Wavelet-transformed contour plots for ruthenium K-edge EXAFS spectra of Bi₂Ru₂O₇ in pristine WE and (b) WE-KOH. The parameters of wavelet-transformed contour plots were $\eta=5$ and $\sigma=1$.

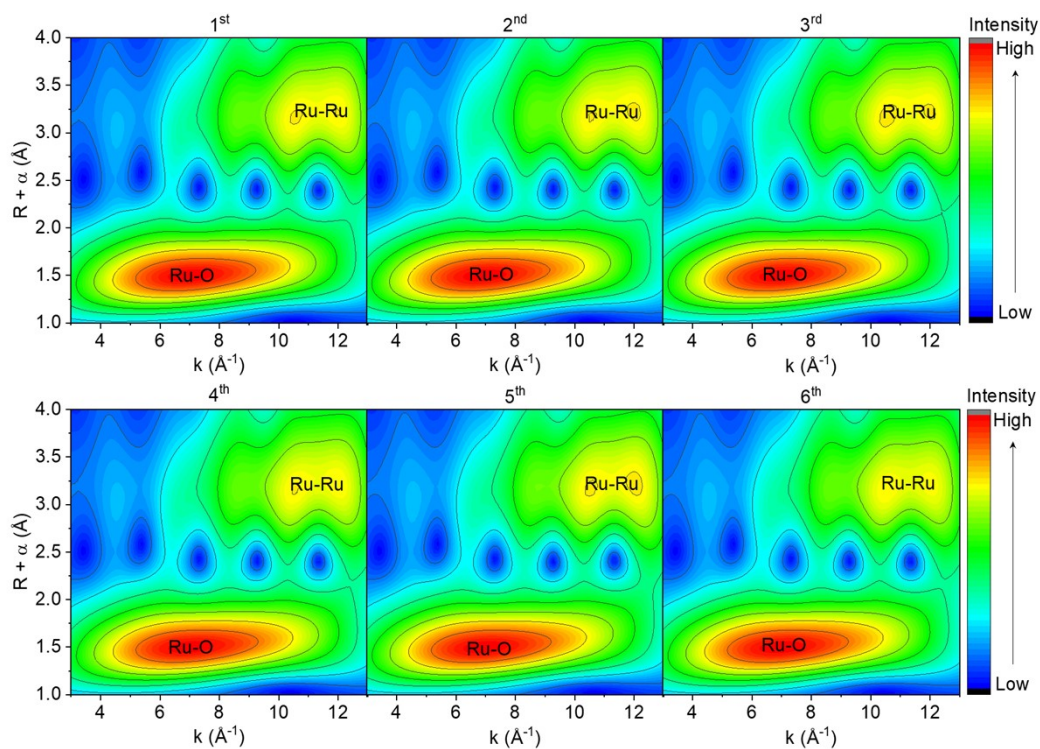


Fig. S14 Wavelet-transformed contour plots for ruthenium K-edge EXAFS spectra of $\text{Bi}_2\text{Ru}_2\text{O}_7$ during OER in the forward sweep of CV test simultaneously with XAS analysis. The parameters of wavelet-transformed contour plots were $\eta=5$ and $\sigma=1$. The CV was recorded between 1.15 V and 1.7 V vs RHE. The scan number of XAS analysis for OER in the forward sweep ranged from 1st to 6th.

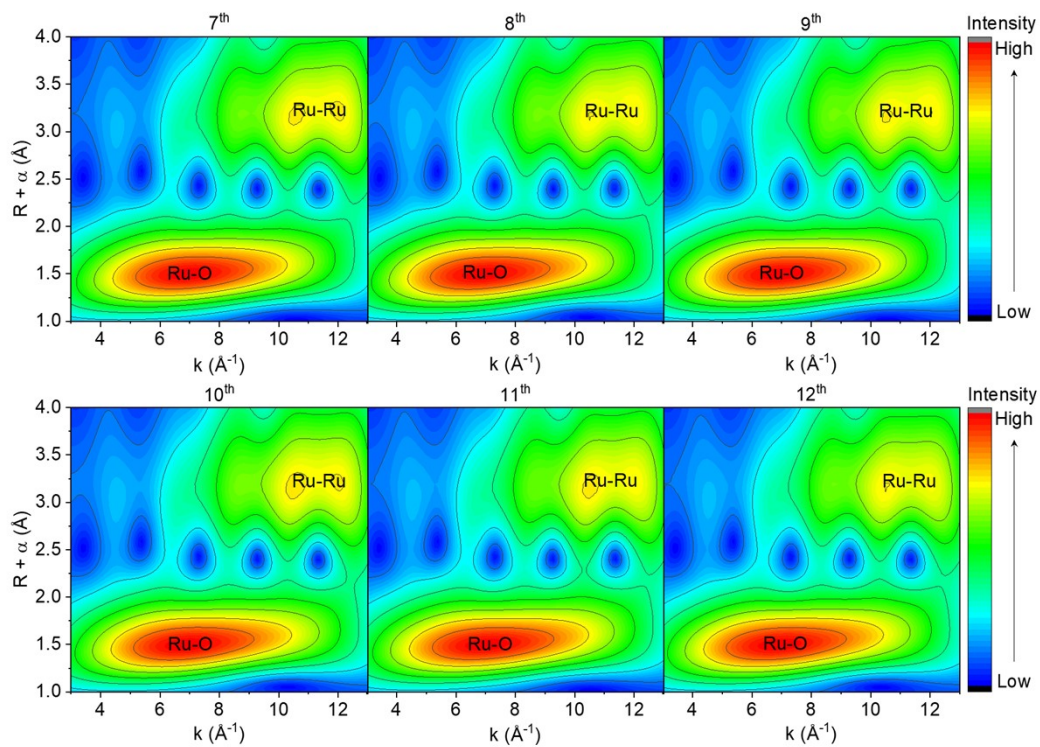


Fig. S15 Wavelet-transformed contour plots for ruthenium K-edge EXAFS spectra of $\text{Bi}_2\text{Ru}_2\text{O}_7$ during OER in the backward sweep of CV test simultaneously with XAS analysis. The parameters of wavelet-transformed contour plots were $\eta=5$ and $\sigma=1$. The CV was recorded between 1.15 V and 1.7 V vs RHE. The scan number of XAS analysis for OER in the backward sweep ranged from 7th to 12th.